Oncogene (2006) 25, 2708–2716

www.nature.com/onc

ORIGINAL ARTICLE

Stability of p21$^{Waf1/Cip1}$ CDK inhibitor protein is responsive to RhoA-mediated regulation of the actin cytoskeleton

ML Coleman[1], RM Densham[2], DR Croft[2] and MF Olson[2]

[1]*The Wellcome Trust Centre for Human Genetics, Oxford, UK and* [2]*The Beatson Institute for Cancer Research, Garscube Estate, Glasgow, UK*

The proto-oncogene Ras GTPase stimulates transcription of p21$^{Waf1/Cip1}$ (p21), which is repressed by the RhoA GTPase. We previously showed that Ras also elevates p21 protein levels by reducing its proteasome-mediated degradation. Therefore, we investigated whether RhoA also influenced p21 protein degradation. Pulse-chase analysis of p21 protein stability revealed that inhibitors of Rho function, which disrupt filamentous actin (F-actin), drastically slowed p21 degradation. Direct F-actin disruption mimicked Rho inhibition to stabilize p21. We found that Rho inhibition, or F-actin disruption, activated the JNK stress-activated protein kinase, and that interfering with JNK signalling, but not p38, abrogated p21 stabilization by Rho inhibition or F-actin-disrupting drugs. In addition, Ras-transformation led to increased constitutive JNK activity that contributed to the elevated p21 protein levels. These data suggest that p21 stability is influenced by a mechanism that monitors F-actin downstream of Rho, and which acts through a pathway involving activation of JNK. These results may have significant implications for therapies that target Rho-signalling pathways to induce p21-mediated cell-cycle arrest.
Oncogene (2006) **25,** 2708–2716. doi:10.1038/sj.onc.1209322; published online 16 January 2006

Keywords: signal transduction; cellular; molecular and tumour biology; guanine nucleotide binding proteins and effectors

Introduction

Ras GTPases play central and critical roles in numerous signal transduction pathways (Coleman *et al*., 2004). They are inactive when GDP-bound and active when GTP-bound; inactivation results from GTP hydrolysis and a return to the inactive GDP-bound state. Ras GTPases were first identified because of their link with human cancer. Specific mutations in each of the three Ras genes, H, K or N-Ras, results in diminished GTPase activity, which converts them into active oncogenes that have been found in a variety of tumour types. Active Ras stimulates a number of effector pathways, one critical pathway being the three-component mitogen activated protein (MAP) kinase cascade consisting of the Raf, MEK and ERK kinases.

Rho GTPases were originally discovered because of their *Ra*s *ho*mology (Coleman *et al*., 2004). To date, 21 Rho GTPases have been described, the most well-characterized being RhoA, Rac1 and Cdc42. Rho GTPases are activated by extracellular signals that promote GDP-GTP exchange; inactivation also occurs through GTP-hydrolysis and a return to the GDP-bound state. Rho proteins were initially shown to regulate the actin cytoskeleton; consequently, they influence cell morphology and motility. However, they also influence gene expression, cell cycle progression and survival, processes that contribute to tumorigenesis. Unlike Ras, where mutations are found in tumours, Rho mutations have not been described, although elevated Rho protein levels are found in many tumours (Sahai and Marshall, 2002).

Cell cycle progression is driven by cyclin-dependent kinases (CDKs) in association with cyclins (Coleman *et al*., 2004). The activities of cyclin–CDK complexes are modulated by two classes of CDK inhibitor (CDKIs). The INK4 CDKI proteins (p15^{INK4b}, p16^{INK4a}, p18^{INK4c} and p19^{INK4d}) sequester CDKs and inhibit the formation of CDK-cyclin complexes, whereas the Cip/Kip CDKIs (p21$^{Waf1/Cip1}$ (p21), p27^{Kip1} (p27) and p57^{Kip2} (p57)) bind to cyclin-CDK complexes. At high levels, p21 and p27 act as potent cyclin E–CDK2 inhibitors, leading to cell-cycle arrest. At lower levels, however, p21 and p27 actually promote the assembly, stability and nuclear retention of cyclin D–CDK4 and cyclin D–CDK6 complexes, which are inefficiently inhibited by associated Cip/Kip proteins. Therefore, the relative levels of cyclins, CDKs and CDKIs determine whether cell-cycle progression will occur. In addition, CDKIs may influence actin cytoskeletal structures and cell motility by attenuating Rho signalling; for example, p27 directly binds and inhibits RhoA (Besson *et al*., 2004), whereas p21 and p57 have been reported to inhibit downstream signalling by inhibiting ROCK (Tanaka *et al*., 2002; Lee and Helfman, 2004) and LIM (Yokoo *et al*., 2003) kinases, respectively.

Correspondence: Dr M Olson, The Beatson Institute for Cancer Research, Garscube Estate, Switchback Road, Glasgow, G61 1BD, UK.
E-mail: m.olson@beatson.gla.ac.uk
Received 15 June 2005; revised 10 October 2005; accepted 11 November 2005; published online 16 January 2006

Despite the robust transforming ability of oncogenic Ras, RhoA inhibition significantly impairs Ras-mediated transformation, and active RhoA cooperates with Raf to promote transformation (Qiu *et al*., 1995). In characterizing Rho and Ras cooperation, we found that Rho suppresses Ras-mediated p21 induction, thereby facilitating cell-cycle progression (Olson *et al*., 1998). Therefore, Rho inhibition may be a good therapeutic target in tumours containing Ras mutations as small variations in p21 may switch it from being a cyclin-CDK assembly factor to an inhibitor of proliferation.

Rho function can be blocked by targeting critical post-translational modifications (Walker and Olson, 2005). The first step is attachment of a 20-carbon geranylgeranyl prenyl group to the Cysteine in the carboxyl-terminal CAAX box by the geranylgeranyl transferase I (GGTase I). GGTase I inhibitors have been developed that efficiently block RhoA processing and consequently lead to p21-mediated cell-cycle arrest (Adnane *et al*., 1998). An alternative is to limit geranylgeranyl pyrophosphate production by inhibiting 3-hydroxy 3-methylglutaryl coenzyme A (HMG-CoA) reductase (Walker and Olson, 2005), which converts HMG-CoA to mevalonate, a five-carbon molecule required for geranylgeranyl pyrophosphate synthesis. HMG-CoA reductase inhibition induces cell-cycle arrest associated with RhoA inactivation and increased p21 levels (Denoyelle *et al*., 2001; Danesh *et al*., 2002; Denoyelle *et al*., 2003). Following RhoA geranylgeranylation, the Rce1 endopeptidase removes the terminal three amino acids; ultimately, the isoprenylated Cysteine is methylated by the isoprenylcysteine carboxyl methyltransferase (ICMT). Genetic inactivation of ICMT inhibited K-Ras and B-Raf transformation of mouse fibroblasts owing to reduced RhoA protein levels and consequent increase in p21 (Bergo *et al*., 2004). These results suggest that targeting these protein-modifying enzymes might effectively block cancer cell replication by inhibiting RhoA and consequently increasing p21 levels.

Given that inhibiting RhoA by a variety of methods results in elevated p21 and cell-cycle arrest, we wished to characterize the Rho-regulated mechanisms that affect p21. We and others previously showed that Rho influences p21 transcription (Adnane *et al*., 1998; Olson *et al*., 1998; Liberto *et al*., 2002; Han *et al*., 2005). However, as p21 is a short-lived protein and by virtue of our previous finding that Ras-induced p21 elevation works principally via protein stabilization (Coleman *et al*., 2003), we wanted to determine whether RhoA regulated p21 by additional mechanisms. These studies could have significant implications for anticancer strategies that work by targeting RhoA function.

Results

Rho regulates p21 protein and mRNA levels in Ras-transformed fibroblasts

Oncogenic transformation induced by highly elevated Ras signalling imposes a selective pressure for increased RhoA-GTP levels (Sahai *et al*., 2001). The selective pressure is applied by Raf/ERK-mediated p21 induction to inhibitory levels, which can be repressed to permissive levels by active RhoA (Olson *et al*., 1998; Sahai *et al*., 2001). Given that elevated p21 levels in Ras-transformed fibroblasts resulted principally from protein stabilization (Coleman *et al*., 2003), we wished to determine whether Rho regulated p21 by post-translational as well as transcriptional mechanisms (Olson *et al*., 1998). RhoA function was inhibited in serum-deprived Ras-transformed Swiss 3T3 fibroblasts (Ras-S3T3; Olson *et al*., 1998) for 16 h with a cell-permeable Tat-fusion form of the *Clostridium botulinum* C3 exoenzyme (Coleman *et al*., 2001), which inactivates RhoA by ADP-ribosylation at Asparagine 41 (Aktories *et al*., 1992). Western blotting revealed that in Tat-C3-treated cells, RhoA was completely ADP-ribosylated as judged by its slower migration, and that C3 treatment increased the expression of p21 (Figure 1a). A similar pattern was observed for p21 mRNA where Tat-C3 treatment increased transcript levels (Figure 1b).

RhoA can be activated by lysophosphatidic acid, a major lipid component of serum (Ridley and Hall, 1992; Ren *et al*., 1999). To determine whether serum would lower p21 protein and/or mRNA in a RhoA-dependent manner, Ras-S3T3 cells were treated with media containing 10% fetal calf serum (FCS) in the presence or absence of Tat-C3. Serum stimulation was Tat-C3 sensitive for repression of p21 protein (Figure 1a, first and third lanes) and mRNA (Figure 1b, first and third lanes), indicating Rho-dependence (Figure 1a and b, third and forth lanes). Consistent with these results, serum-stimulation of Ras-S3T3 cells activated RhoA (Figure 1c) as determined by measuring GTP-bound Rho by affinity purification using the Rhotekin Rho-binding domain (Coleman *et al*., 2001).

Densitometric quantification from two independent experiments indicated that p21 protein levels were more substantially reduced by FCS-stimulation ($\sim$2.8 fold) than mRNA levels ($\sim$1.7 fold; Figure 1d). Similarly, Rho inhibition in the presence of FCS increased p21 protein levels by $\sim$3.5-fold compared to the $\sim$1.7-fold increase in p21 mRNA. The differences between p21 mRNA and protein levels suggested that post-transcriptional mechanisms possibly contribute to Rho-mediated p21 regulation.

Rho regulates p21 protein stability

To determine whether RhoA regulates p21 protein stability, we used a radioactive pulse-chase method we previously employed to examine Ras-induced p21 stabilization (Coleman *et al*., 2003). NIH 3T3 cells were transfected with FLAG-epitope-tagged p21, without or with Myc-epitope-tagged C3, and incubated with ^{35}S-labelled methionine/cysteine followed by a chase with excess unlabelled methionine/cysteine for up to 4 h (Figure 2a). Radiolabelled transfected p21 was immunoprecipitated with FLAG monoclonal antibody, electrophoresed and transferred to membranes; the radioactivity present at each point was measured by phosphorimaging with results presented as the average

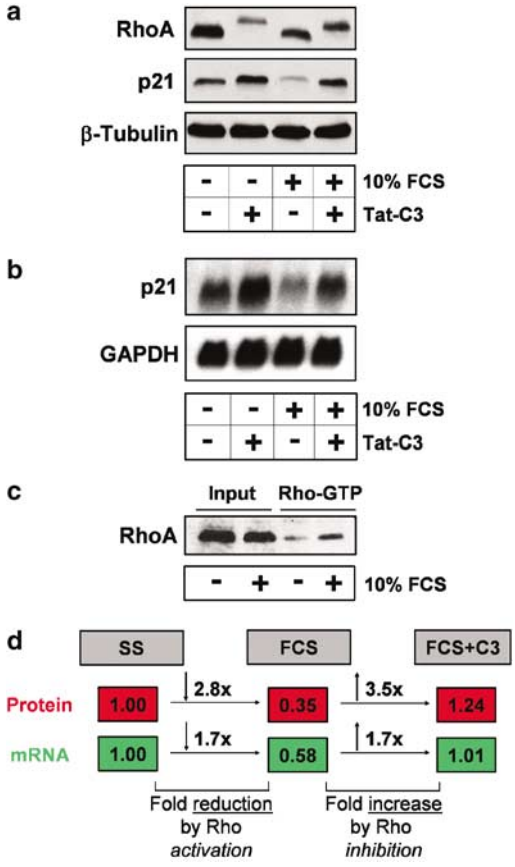

Figure 1 Rho regulation of p21 protein and mRNA. (**a**) Ras-S3T3 cells were incubated for 16 h in the presence or absence of 10% FCS and 0.5 μM recombinant Tat-C3. Extracts were Western blotted with indicated antibodies. β-Tubulin controlled for loading. (**b**) Ras-S3T3 cells were treated as described before isolating RNA and Northern blotting with indicated probes. (**c**) Rho activation by FCS. Ras-S3T3 cells were serum-starved and stimulated with 10% FCS where indicated for 1 min before purifying Rho-GTP from cell lysates using the Rhotekin Rho-binding domain (**d**) Quantitative comparison of changes in p21 protein and mRNA levels upon Rho activation and inhibition. p21 protein levels were quantified by densitometry of Western blots. mRNA was quantified by phosphorimager analysis of ^{32}P-labelled p21 DNA probe hybridized to Northern blots. Boxed numbers represent expression levels relative to serum-starved (SS) cells and are the average of two independent experiments.

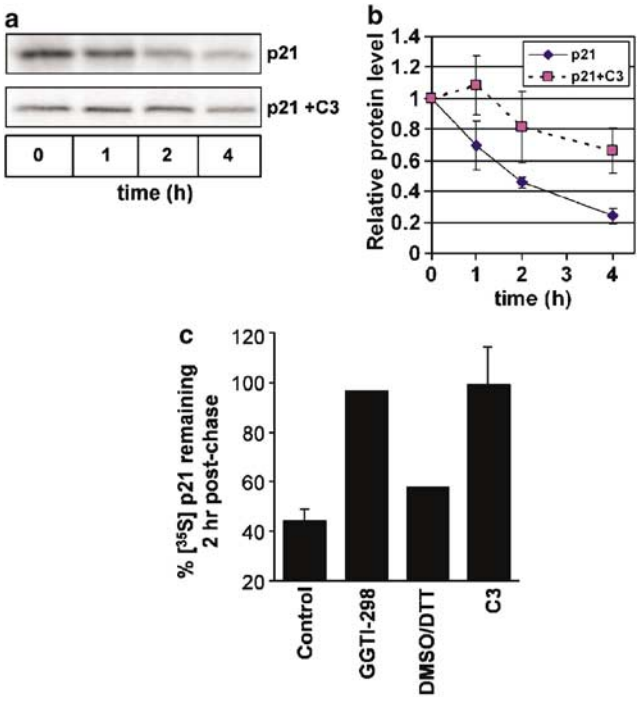

Figure 2 Pulse-chase analysis of p21 stabilization following Rho inhibition. (**a**) NIH 3T3 cells were transfected with p21 or with p21 plus C3, deprived of serum overnight and then incubated with ^{35}S-labelled methionine/cysteine for 1 h, followed by a chase with excess unlabelled methionine/cysteine for the indicated times. Labelled p21 was immunoprecipitated from equal quantities of cell lysates. Although p21 transfected alone was degraded over the 4 h time period, coexpression with C3 resulted in significant protein stabilization. (**b**) Labelled p21 from three independent experiments was quantitated by phosphorimager analysis and the average percentages and standard errors for each time point relative to $t=0$ for p21 alone or p21 plus C3 are presented. Coexpression with C3 increased the amount of p21 remaining at all time points. (**c**) The effects of C3 can be mimicked by inhibiting geranylgeranyl transferase I activity with GGTI-298. Cells were transfected and, where indicated, were left untreated or treated with 10 μM GGTI-298 or vehicle control for 20 h, labelled with [^{35}S] and p21 immunoprecipitated at the beginning of the chase or 2 h post-chase. For comparative purposes, data are represented as percent ^{35}S-labelled p21.

percentage of ^{35}S-labelled p21 remaining relative to the amount at $t=0$ (Figure 2b). When transfected alone, p21 levels declined over time; in contrast, C3 coexpression slowed p21 turnover (Figure 2a and b).

For further radioactive pulse-chase experiments, we used a 2 h time point, which is within the linear p21 degradation phase (Figure 2b). We examined whether inhibiting RhoA with the GGTase I inhibitor GGTI-298 (Adnane *et al*., 1998) would also stabilize p21. GGTI-298 treatment was reported to induce cell-cycle arrest by increasing p21 levels, which was attributed to RhoA inhibition and reduced RhoA-mediated repression of p21 transcription (Adnane *et al*., 1998). Transfected cells were serum-starved and incubated without or with GGTI-298 for 20 h. Pulse-chase analysis revealed that either GGTI-298 treatment or cotransfection with C3 plasmid stabilized p21, whereas the drug vehicle was without effect (Figure 2c). These data indicate that p21 stabilization is independent of the method of Rho inhibition.

To determine whether C3-induced p21 stabilization was due to ADP-ribosylation and inhibition of Rho, we performed a 'rescue' experiment using an activated RhoA (RhoA V14) in which the Glutamine at position 41 was mutated to a non-ADP-ribosylatable Isoleucine (RhoA V14I41; Hill *et al*., 1995). Coexpression of RhoA V14I41 with C3 blocked p21 stabilization (Figure 3a), although RhoA V14I41 (Figure 3a) or RhoA V14 expression (Figure 3b) did not accelerate p21 turnover. In contrast, active Rac1 V12 stabilized p21, suggesting that basal RhoA activity, which can be inhibited by C3 or GGTI-298, is sufficient for maximal p21 degradation,

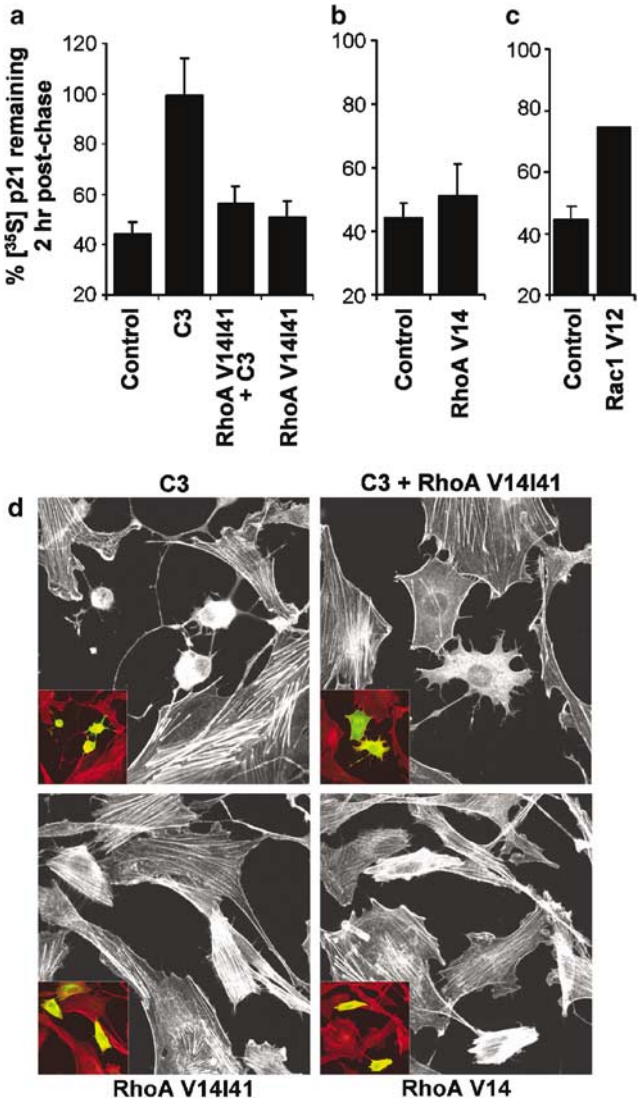

Figure 3 Effect of activated Rho on p21 stability. (**a**) An activated RhoA mutant that cannot be ADP-ribosylated reverses C3-induced p21 stabilization. NIH 3T3 cells were transfected with Flag-p21, Myc-C3 and/or the C3-insensitive mutant Myc-RhoA V14I41 and pulse-chased as described. (**b**) Activated RhoA does not stimulate p21 degradation. NIH 3T3 cells were transfected with Flag-p21 and Myc-RhoA V14 as indicated and pulse-chased as described. (**c**) Activated Rac1 stabilizes p21. NIH 3T3 cells were transfected with Flag-p21 and Myc-Rac1 V12 as indicated and pulse-chased as described. (**d**) Changes to the actin cytoskeleton and cell morphology induced by C3 and GTPase-deficient RhoA. NIH 3T3 cells were transfected with Myc-C3, Myc-RhoA V14 and/or the C3-insensitive Myc-RhoA V14I41 and serum-starved overnight before staining for Myc (FITC) and F-actin (Texas Red) as described. Inset panels indicate transfected cells (green).

consistent with the presence of Rho-dependent filamentous actin (F-actin). These data indicate that p21 stabilization by C3 is specifically due to ADP-ribosylation and inactivation of Rho, and not from 'off-target' actions.

To determine how p21 stabilization correlated with effects on the actin cytoskeleton, NIH 3T3 cells were transfected with Myc-tagged C3, RhoA V14, or RhoA V14I41 individually, or with C3 plus RhoA V14I41, before serum-starvation, fixation and staining for Myc-epitope expression (green in Figure 3d inset panels) and F-actin structures (white in Figure 3d large panels, red in inset panels). As shown previously (Chardin *et al*., 1989; Paterson *et al*., 1990; Ridley and Hall, 1992), C3 disrupted organized actin fibres resulting in cell rounding (Figure 3d). Co-expression of C3 with active RhoA V14I41 prevented cell rounding and restored normal cortical actin structures with diffuse cytoplasmic F-actin staining; however, central actin fibres were not fully restored. The inability of RhoA V14I41 to fully rescue central actin fibres possibly reflects the 'dominant-negative' inhibitory effect of ADP-ribosylated endogenous Rho (Paterson *et al*., 1990; Ridley and Hall, 1992). As expected, RhoA V14 and RhoA V14I41 increased contractile F-actin fibres (Figure 3d).

F-actin destabilizing drugs mimic Rho inhibition on p21 stability

The most well-characterized Rho GTPase function is the regulation of the actin cytoskeleton. As p21 stabilization by C3 was associated with F-actin loss, we next determined whether direct F-actin disruption would mimic Rho inhibition. Cells were treated with two commonly used F-actin destabilizing drugs during pulse-chase analysis: Latrunculin B (LTB, from *Latrunculia magnificans*), which binds G-actin monomers and blocks polymerization into filaments (Spector *et al*., 1983) and Cytochalasin D (CTD, from *Zygusporium mansonii*), which caps F-actin and stimulates G-actin ATP hydrolysis (Sampath and Pollard, 1991). LTB or CTD treatment had significant effects on F-actin structures and distribution of the focal-adhesion protein paxillin (Figure 4a). Untreated serum-starved cells had numerous stress fibres with paxillin at terminal focal adhesions (Figure 4a, left panel). CTD-treatment efficiently disrupted central actin fibres and decreased overall F-actin levels without affecting cortical actin; consequently, cells remained adherent and well spread (Figure 4a, middle panel). Paxillin-containing focal adhesions were significantly reduced but not entirely eliminated by CTD. LTB treatment caused dramatic morphological changes: cells rounded with long projections, and lost central actin fibres, cortical actin structures and focal adhesions (Figure 4a, right panel). Incubation of p21-transfected NIH 3T3 cells with either LTB or CTD increased radiolabelled p21 levels remaining 2 h post-chase, relative to untreated samples (Figure 4b). Therefore, F-actin may be the critical target downstream of Rho involved in regulating p21 stability. However, the ability of these drugs to destabilize F-actin and disrupt focal adhesions, but not the degree to which they alter cell morphology, was associated with p21 stabilization.

F-actin disruption by C3 or CTD has been reported to activate the stress-activated protein kinases (SAPK) JNK and p38 (Beltman *et al*., 1999; Yujiri *et al*., 1999; Subbaramaiah *et al*., 2000). JNK and p38 have been implicated in regulating the stability of various proteins including p21 (Fuchs *et al*., 1998; Kim *et al*., 2002).

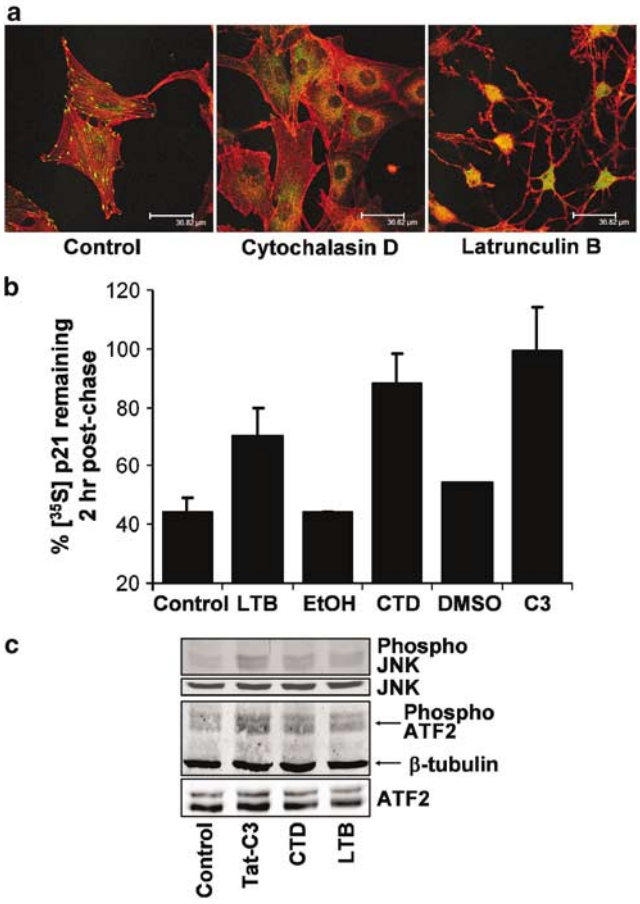

Figure 4 Actin disruption stabilizes p21 and activates JNK. (**a**) Disruption of the actin cytoskeleton by actin-binding drugs. Serum-starved NIH 3T3 cells were treated with either 25 nM Latrunculin B (LTB) or 200 nM Cytochalasin D (CTD) for 3 h before staining for F-actin. (**b**) NIH 3T3 cells were transfected with p21, serum-starved overnight and treated with 25 nM LTB, LTB vehicle (0.0025% ethanol (EtOH)), 200 nM CTD or CTD vehicle control (0.02% DMSO) during the pulse-chase procedure. Data for C3 cotransfection is shown for comparison. (**c**) JNK activation and ATF2 phosphorylation induced by actin disruption. NIH 3T3 cells were treated with Tat-C3, CTD or LTB at the concentrations used above for 2 h, then Western blotted with indicated antibodies.

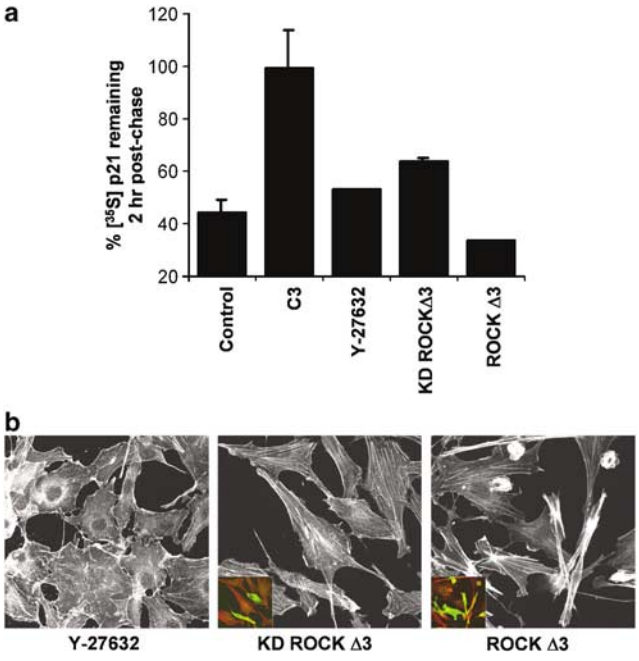

Figure 5 ROCK does not mediate Rho regulation of p21. (**a**) NIH 3T3 cells were transfected with Flag-p21 alone or with Myc-C3, dominant-negative KD ROCKΔ3 or active ROCKΔ3, left untreated or treated with 10 μM Y-27632 for 2 h, and then pulse-chased as described. Inhibition of ROCK with Y-27632 or KD ROCKΔ3 had a small stabilizing effect whereas active ROCKΔ3 slightly promoted p21 degradation. (**b**) Actin-staining revealed that Y-27632 eliminated central actin fibres but stimulated membrane ruffling. Expression of KD ROCKΔ3 had little effect, whereas active ROCKΔ3 induced the formation of prominent stellate actin bundles.

Therefore, we Western blotted extracts from NIH 3T3 cells treated for 2 h with Tat-C3, CTD or LTB for the presence of active phospho-JNK as well as for phosphorylation of the ATF2 transcription factor, a well-characterized JNK substrate. Each of these treatments increased phospho-JNK and phospho-ATF2 levels without affecting total JNK, ATF2 or β-tubulin levels (Figure 4c). The potency of JNK activation and ATF2 phosphorylation paralleled p21 stabilization with C3 > CTD > LTB.

ROCK contributes little to p21 stabilization

We next examined whether the Rho effector ROCK contributed to p21 regulation. ROCK 1 and 2 are activated by Rho and regulate actin structures by several means, largely by increasing actin filament bundling with myosin and promoting actin-myosin contractility (Riento and Ridley, 2003). NIH 3T3 cells were transfected with p21 alone, or in combination with C3, kinase-inactive (K105A) dominant-negative ROCK I (KD ROCKΔ3, (Itoh *et al*., 1999)) or active ROCK I (ROCKΔ3, (Itoh *et al*., 1999)), then left either untreated or treated with ROCK inhibitor Y-27632 (Uehata *et al*., 1997) as indicated. Pulse-chase analysis indicated that KD ROCKΔ3 or Y-27632 only slightly affected p21 stability (Figure 5a). Conversely, expression of active ROCKΔ3 slightly increased p21 degradation. Y-27632-treated cells lost central actin fibres but had increased peripheral ruffles while retaining cortical and diffuse cytoplasmic F-actin (Figure 5b). However, F-actin structures in KD ROCKΔ3-expressing cells were not significantly affected (Figure 5b). Consistent with previous reports (Sahai *et al*., 2001), active ROCKΔ3 induced large stellate actin bundles. These results suggest that p21 regulation is Rho-dependent but largely ROCK-independent, although ROCK may indirectly influence p21 by indirectly affecting actin-myosin bundling and F-actin stability.

C3- and CTD-induced p21 stabilization are JNK-dependent

Given that actin disruption activated JNK (Figure 4c), we examined whether SAPKs contributed to p21

stabilization by C3 or CTD using the p38 inhibitor SB203580 (SB) or a dominant-negative (K129R) version SEK1 (DN SEK), the upstream JNK-activating kinase (Sanchez *et al*., 1994). NIH 3T3 cells were transfected with p21 alone, with p21 plus C3, with DN SEK, or with a combination of p21/C3/DN SEK. Transfected cells were serum-starved overnight before treating with the p38 SAPK inhibitor SB203580 and/or CTD as indicated (Figure 6a). Whereas the p38 inhibitor SB203580 did not prevent C3 or CTD from increasing p21 stability, dominant-negative SEK antagonized p21 stabilization (Figure 6a). We further examined these results by expressing the SAPK-specific dual-specificity phosphatase DUSP8 (Muda *et al*., 1996) to inactivate JNK. Although DUSP8 alone did not increase p21 degradation, CTD-induced stabilization was prevented by DUSP8 (Figure 6b). Finally, we found that the JNK inhibitor SP600125 (Bennett *et al*., 2001) reversed Tat-C3-induced p21 stabilization (Figure 6c) by measuring p21 levels remaining 2 h after emetine-induced protein synthesis inhibition. These results indicate that JNK contributed to p21 stabilization by C3- or CTD-mediated F-actin disruption.

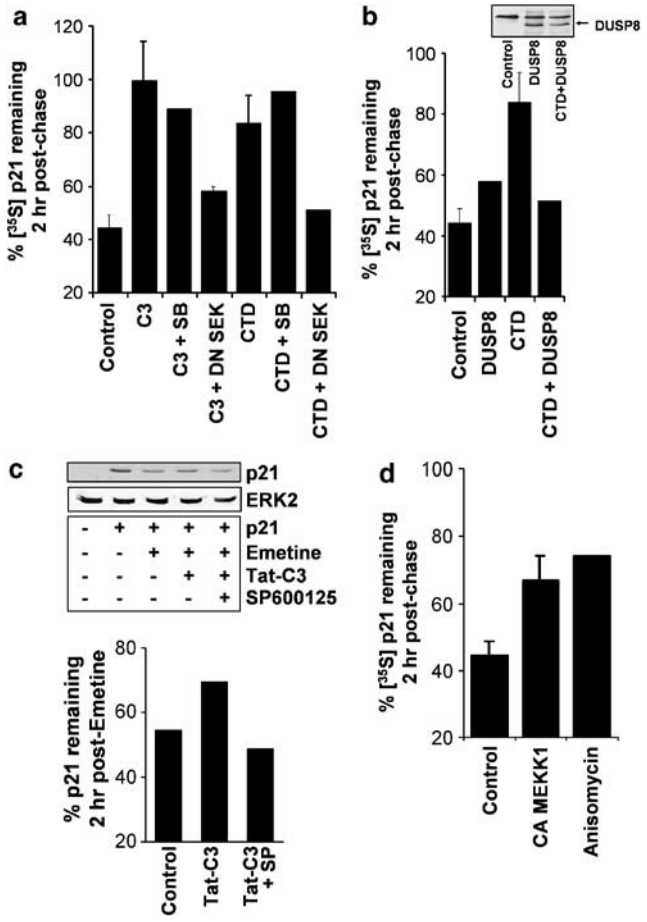

Figure 6 C3 and Cytochalasin D-induced p21 stability is dependent on JNK, but not p38 SAPK activation. (**a**) NIH 3T3 cells were transfected with p21, Myc-C3 or a dominant-negative SEK mutant, Myc-SEK K129R (DN SEK) as indicated, and the following day pulse-chased in the presence or absence of 200 nM Cytochalasin D (CTD) or 10 μM SB203580 (SB) as indicated. (**b**) Inhibition of JNK activity by overexpression of a JNK-phosphatase reduced p21 turnover induced by actin disruption. NIH 3T3 were transfected with p21, either with or without a *myc*-tagged version of the dual-specificity phosphatase DUSP8, then left untreated or treated with 200 nM CTD during the pulse-chase assay. Inset panel shows expression of *myc*-tagged DUSP8 in transfected cells. (**c**) Treatment with a JNK-selective inhibitor reduced p21 turnover following Rho inhibition. NIH 3T3 cells were transfected with p21 as indicated. Cells were treated for 2 h with 20 μM emetine to inhibit protein synthesis, 0.5 μM Tat-C3 to inhibit Rho and 30 μM SP600125 to inhibit JNK as indicated. (**d**) JNK activation is sufficient to reduce p21 turnover. NIH 3T3 cells were transfected with p21 without or with constitutively active MEKK1 (CA MEKK1), serum-starved overnight and pulse-chased in the presence of 0.1 mM Anisomycin as indicated.

JNK activation promotes p21 stability

Given that JNK activity was required for p21 stabilization following F-actin disruption, JNK activation independent of C3 or CTD might be sufficient to inhibit p21 degradation. NIH 3T3 cells were transfected with C3 alone or with a constitutively active fragment of the upstream activating kinase of the SEK/JNK pathway, MEKK1 (CA MEKK1; Olson *et al*., 1995). Pulse-chase analysis indicated that MEKK1 stabilized p21 (Figure 6d). Treatment with anisomycin, a cell-permeable JNK activator (Meier *et al*., 1996) also reduced p21 turnover (Figure 6d). These data are consistent with the model that JNK mediates the p21 stabilization that results from C3- and CTD-induced F-actin disruption.

Ras activation of JNK contributes to p21 stabilization

We previously reported that the elevated p21 in Ras-transformed fibroblasts resulted principally from protein stabilization, owing to cyclin D1-mediated sequestration from the proteasome complex (Coleman *et al*., 2003). However, given that Ras has been reported to activate JNK (Derijard *et al*., 1994; McCarthy *et al*., 1995), the possibility remained that constitutively elevated JNK activity contributed to Ras-induced p21 stabilization. Ras-transformed Swiss 3T3 fibroblasts were found to have increased levels of Ras, p21, phospho-JNK and phospho-ATF2 when compared to parental cells, whereas β-tubulin, JNK and ATF2 levels were not different (Figure 7a). These results indicate that Ras-transformation and increased p21 were associated with JNK activation. We next examined whether the JNK inhibitor SP600125 would reduce basal p21 levels in Ras-transformed cells and reverse the p21-elevating effect of Rho inhibition by Tat-C3. SP600125 treatment for 2 h reduced basal phospho-ATF2 and p21 levels (Figure 7b). Tat-C3 increased phospho-JNK, phospho-ATF2 and p21 levels, whereas SP600125 inhibited ATF2 phosphorylation and restricted p21 elevation. Expression of β-tubulin, JNK and ATF2 remained constant, although a shift in ATF2 mobility, consistent with phosphorylation, was observed with Tat-C3 treatment. Cyclin D1 expression was not affected by Tat-C3, indicating that increased p21 did not result from cyclin D1-mediated sequestration (Coleman *et al*., 2003). These results indicate that Ras-induced p21 elevation possibly has the additional component of JNK-mediated stabilization, and that

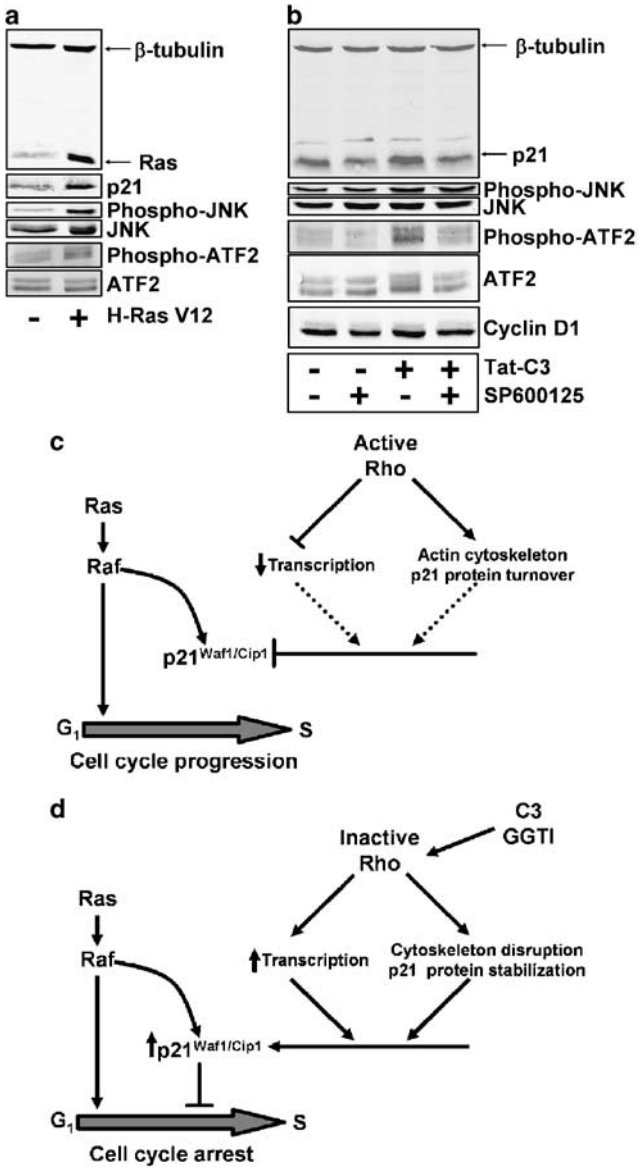

Figure 7 Rho inhibition results in $p21^{Waf1/Cip1}$ elevation by transcriptional and post-translational mechanisms. (**a**) Parental and Ras-transformed Swiss 3T3 cells were blotted as indicated. Ras-transformation led to elevated p21 associated with increased basal JNK activity and ATF2 phosphorylation. (**b**) Ras-transformed Swiss 3T3 cells were untreated or Tat-C3 treated, either without or with JNK inhibitor SP600125 as indicated. JNK inhibition reduced basal and Tat-C3-induced ATF2 phosphorylation and p21 elevation. (**c**) Ras signalling via Raf induces cell-cycle progression if active Rho represses p21 expression to permissive levels. (**d**) Rho inactivation allows for increased Ras-induced p21 transcription whereas disruption of the actin cytoskeleton results in stabilization of p21 protein. The elevated p21 blocks Ras-induced cell-cycle progression.

JNK activity can be further stimulated by Rho inhibition leading to additional p21 accumulation.

Discussion

High-intensity Ras/Raf/MAPK activation can elicit cell-cycle arrest associated with growth inhibitory p21 levels (Lloyd *et al*., 1997; Pumiglia and Decker, 1997; Woods *et al*., 1997; Olson *et al*., 1998), yet Ras-transformed fibroblasts are able to overcome this arrest (Sahai *et al*., 2001). One explanation that reconciles these observations is that sustained Raf activation selects for cells with elevated active Rho that represses p21 accumulation (Sahai *et al*., 2001). Consistent with this model, p21 mRNA levels were not elevated in Ras-transformed Swiss 3T3 cells unless Rho activity was inhibited (Figure 1 and (Coleman *et al*., 2003)). Instead, enhanced p21 protein stability mediated by Ras-induction of cyclin D1, which sequesters p21 from proteasome-mediated degradation, is the principal contributory factor (Coleman *et al*., 2003). Therefore, cells with high Rho activity repress the transcriptional component sufficiently such that cell-cycle progression is permitted, and these selected cells expand into a transformed population (Figure 7c).

Given that Ras regulation of p21 has transcriptional and post-transcriptional components, we wished to determine whether Rho also influenced p21 levels through multiple mechanisms. We found that Rho inhibition in Ras-transformed cells resulted in elevation of p21 protein levels greater than the increase in p21 mRNA, suggesting an additional post-transcriptional component. Through pulse-chase radiolabelling experiments, we determined that Rho inhibition with C3 exoenzyme, or by inhibiting geranylgeranyl transferase I activity, stabilized p21 protein. As the best-characterized Rho function is regulation of the actin cytoskeleton, we tested whether F-actin disruption would inhibit p21 degradation. Indeed, decreased F-actin levels induced by LTB or CTD (Figure 4a) was sufficient to stabilize p21 (Figure 4b). In contrast, actin-myosin bundling and contractility regulated by ROCK appears to contribute only slightly, if at all, to Rho regulation of p21 (Figure 5).

Given that F-actin disruption induced by C3, LTB or CTD resulted in JNK activation (Figure 4c), we tested whether JNK signalling contributed to p21 stabilization. Inhibition of JNK by dominant-negative SEK, expression of DUSP8 or SP600125 treatment reduced C3- or CTD-induced p21 stabilization (Figure 6a-c). In addition, direct activation of JNK by MEKK1 or anisomycin also stabilized p21 (Figure 6d), whereas JNK inhibition with SP600125 in Ras-transformed cells reduced the elevated p21 associated with increased JNK activity in both untreated and Tat-C3-treated cells (Figure 7a-b). These data suggest that there is a mechanism that senses decreased F-actin, or increased G-actin, which signals through the JNK pathway to regulate p21 stability. Given that active Rac1 both increases F-actin (Ridley *et al*., 1992) and potently activates JNK (Olson *et al*., 1995), the stabilization of p21 by Rac1 V12 (Figure 3c) suggests that JNK activity dominates over the actin-sensing mechanism to influence p21 stability.

Although previous studies have concentrated on the role of Rho in regulating p21 transcription (Adnane *et al*., 1998; Olson *et al*., 1998; Liberto *et al*., 2002; Han *et al*., 2005), it is likely that methods of blocking

Rho function, in addition to C3 or GGTI-298 including inhibition of HMG-CoA reductase (Denoyelle *et al*., 2001; Danesh *et al*., 2002; Denoyelle *et al*., 2003) or ICMT (Bergo *et al*., 2004), also elevate p21 through post-translational stabilization as well as increased transcription. In contrast to the p21 elevation in Ras-transformed cells where stabilization was the principal mechanism (Coleman *et al*., 2003), our results indicate that both increased transcription and protein stabilization contribute to p21 elevation following Rho inhibition. It is unclear whether specifically targeting either transcription or protein stabilization would be sufficient to induce cell-cycle arrest as efficiently as Rho inhibition. These results, therefore, have significant implications for targeting strategies for cancer chemotherapy.

An intact actin cytoskeleton and normal Rho signalling are associated with cell proliferation, whereas Rho inhibition and loss of cytoskeletal integrity are associated with cell-cycle arrest (Olson *et al*., 1995; Bohmer *et al*., 1996; Assoian and Zhu, 1997; Olson *et al*., 1998; Reshetnikova *et al*., 2000; Sahai *et al*., 2001; Huang and Ingber, 2002). Although the mechanism by which F-actin influences p21 levels has not been extensively studied, the growth arrest of adherent cells placed in suspension has been associated with actin disruption and high p21 levels (Fang *et al*., 1996; Zhu *et al*., 1996; Bottazzi *et al*., 1999). Cell cycle checkpoints responsive to F-actin disruption have been characterized in yeast (Lew, 2003). F-actin disruption in *Schizosaccharomyces pombe* leads to cell-cycle arrest owing to stabilization of the inhibitory kinase Swe1p, which inhibits the CDK Cdc28p (Harrison *et al*., 2001). In addition, activation of the SAPK Hog1 in *Saccharomyces cerevisiae* arrests cells because of the stabilization of the CDK inhibitor Sic1 and the consequent inhibition of the CDK Cdc28 (Escote *et al*., 2004). Therefore, p21 may contribute to a similar checkpoint in mammalian cells that responds to changes in F-actin levels. The recurrence of cell-cycle checkpoints that monitor the actin cytoskeleton highlights the importance of restricting cell proliferation to the correct environmental context. Loss of these checkpoints may permit anchorage-independent cell proliferation, a hallmark of cancer.

Materials and methods

Cell culture
NIH 3T3 and Swiss 3T3 mouse fibroblasts were grown at 10% CO_2 in Dulbecco's Modified Eagles Medium (DMEM; GibcoBRL) supplemented with penicillin and streptomycin and 10% (v/v) fetal calf serum (Swiss 3T3; PAA Labs) or donor calf serum (NIH 3T3; GibcoBRL). Serum starvation involved rinsing cells once in serum-free DMEM before incubation with serum-free media for $\sim$16 h.

Immunofluorescence
Cells were fixed and stained for immunofluorescence as previously described (Coleman *et al*., 2001). Paxillin antibody was from Sigma.

Northern blots
RNA electrophoresis and Northern blotting were performed as previously described (Coleman *et al*., 2003). DNA probes for p21 mRNA were PCR-amplified from Swiss 3T3 cDNA using the primers: p21 forward CAATCCTGGTGATGTCCGACCTG and p21 reverse GCAGAAGACCAATCTGCGCTTGG. GAPDH probe was full-length coding sequence cDNA (G. Mavria, Institute of Cancer Research, London). Radioactive membranes were exposed to a phosphorimager screen (Molecular Dynamics) for 2–20 h before scanning with a Storm 860 PhosphorImager and analysis with Imagequant software (Molecular Dynamics).

Western blots
Western blotting was performed as previously described (Coleman *et al*., 2003). HRP-conjugated secondary antibodies were detected with Enhanced Chemiluminescence (ECL; Amersham). Alternatively, Alexa-Fluor680 (Molecular Probes or IRDye800 (Rockland) conjugated secondary antibodies were detected by infrared imaging (Li-Cor Odyssey).

Pulse-chase analysis
Pulse-chase experiments were performed in NIH 3T3 cells as previously described (Coleman *et al*., 2003). Following SDS–PAGE, transfer to PVDF membrane and exposure to a phosphorimager screen, ^{35}S-labelled p21 was quantified using Imagequant software. Alternatively, NIH3T3 cells were transfected with FLAG-p21 and grown in serum-free media for 16 h before treatment with the protein synthesis inhibitor emetine (20 μM) and combinations of Tat-C3 (0.5 μM) and SP600125 (30 μM) as indicated for 2 h. Whole cell lysates were probed for p21 and ERK2, and quantified by infrared imaging as described above.

Acknowledgements

We thank S. Sebti (University of South Florida, Tampa, Florida) for the gift of GGTI-298. This study was supported by Cancer Research UK and a National Cancer Institute grant R01 CA030721 to M. Olson.

References

Adnane J, Bizouarn FA, Qian Y, Hamilton AD, Sebti SM. (1998). *Mol Cell Biol* **18**: 6962–6970.
Aktories K, Mohr C, Koch G. (1992). *Curr Top Microbiol Immunol* **175**: 115–131.
Assoian RK, Zhu X. (1997). *Curr Opin Cell Biol* **9**: 93–98.
Beltman J, Erickson JR, Martin GA, Lyons JF, Cook SJ. (1999). *J Biol Chem* **274**: 3772–3780.
Bennett BL, Sasaki DT, Murray BW, O'Leary EC, Sakata ST, Xu W, Leisten JC *et al*. (2001). *Proc Natl Acad Sci USA* **98**: 13681–13686.
Bergo MO, Gavino BJ, Hong C, Beigneux AP, McMahon M, Casey PJ *et al*. (2004). *J Clin Invest* **113**: 539–550.
Besson A, Gurian-West M, Schmidt A, Hall A, Roberts JM. (2004). *Genes Dev* **18**: 862–876.
Bohmer RM, Scharf E, Assoian RK. (1996). *Mol Biol Cell* **7**: 101–111.
Bottazzi ME, Zhu X, Bohmer RM, Assoian RK. (1999). *J Cell Biol* **146**: 1255–1264.
Chardin P, Boquet P, Madaule P, Popoff MR, Rubin EJ, Gill DM. (1989). *EMBO J* **8**: 1087–1092.

Coleman ML, Marshall CJ, Olson MF. (2003). *EMBO J* **22**: 2036–2046.
Coleman ML, Marshall CJ, Olson MF. (2004). *Nat Rev Mol Cell Biol* **5**: 355–366.
Coleman ML, Sahai EA, Yeo M, Bosch M, Dewar A, Olson MF. (2001). *Nat Cell Biol* **3**: 339–345.
Danesh FR, Sadeghi MM, Amro N, Philips C, Zeng L, Lin S *et al*. (2002). *Proc Natl Acad Sci USA* **99**: 8301–8305.
Denoyelle C, Albanese P, Uzan G, Hong L, Vannier JP, Soria J *et al*. (2003). *Cell Signal* **15**: 327–338.
Denoyelle C, Vasse M, Korner M, Mishal Z, Ganne F, Vannier JP *et al*. (2001). *Carcinogenesis* **22**: 1139–1148.
Derijard B, Hibi M, Wu IH, Barrett T, Su B, Deng T *et al*. (1994). *Cell* **76**: 1025–1037.
Escote X, Zapater M, Clotet J, Posas F. (2004). *Nat Cell Biol* **6**: 997–1002.
Fang F, Orend G, Watanabe N, Hunter T, Ruoslahti E. (1996). *Science* **271**: 499–502.
Fuchs SY, Fried VA, Ronai Z. (1998). *Oncogene* **17**: 1483–1490.
Han S, Sidell N, Roman J. (2005). *Cancer Lett* **219**: 71–81.
Harrison JC, Bardes ES, Ohya Y, Lew DJ. (2001). *Nat Cell Biol* **3**: 417–420.
Hill CS, Wynne J, Treisman R. (1995). *Cell* **81**: 1159–1170.
Huang S, Ingber DE. (2002). *Exp Cell Res* **275**: 255–264.
Itoh K, Yoshioka K, Akedo H, Uehata M, Ishizaki T, Narumiya S. (1999). *Nat Med* **5**: 221–225.
Kim GY, Mercer SE, Ewton DZ, Yan Z, Jin K, Friedman E. (2002). *J Biol Chem* **277**: 29792–29802.
Lee S, Helfman DM. (2004). *J Biol Chem* **279**: 1885–1891.
Lew DJ. (2003). *Curr Opin Cell Biol* **15**: 648–653.
Liberto M, Cobrinik D, Minden A. (2002). *Oncogene* **21**: 1590–1599.
Lloyd AC, Obermuller F, Staddon S, Barth CF, McMahon M, Land H. (1997). *Genes Dev* **11**: 663–677.
McCarthy SA, Samuels ML, Pritchard CA, Abraham JA, McMahon M. (1995). *Genes Dev* **9**: 1953–1964.
Meier R, Rouse J, Cuenda A, Nebreda AR, Cohen P. (1996). *Eur J Biochem* **236**: 796–805.
Muda M, Theodosiou A, Rodrigues N, Boschert U, Camps M, Gillieron C *et al*. (1996). *J Biol Chem* **271**: 27205–27208.
Olson MF, Ashworth A, Hall A. (1995). *Science* **269**: 1270–1272.
Olson MF, Paterson HF, Marshall CJ. (1998). *Nature* **394**: 295–299.
Paterson HF, Self AJ, Garrett MD, Just I, Aktories K, Hall A. (1990). *J Cell Biol* **111**: 1001–1007.
Pumiglia KM, Decker SJ. (1997). *Proc Natl Acad Sci USA* **94**: 448–452.
Qiu RG, Chen J, McCormick F, Symons M. (1995). *Proc Natl Acad Sci USA* **92**: 11781–11785.
Ren XD, Kiosses WB, Schwartz MA. (1999). *EMBO J* **18**: 578–585.
Reshetnikova G, Barkan R, Popov B, Nikolsky N, Chang LS. (2000). *Exp Cell Res* **259**: 35–53.
Ridley AJ, Hall A. (1992). *Cell* **70**: 389–399.
Ridley AJ, Paterson HF, Johnston CL, Diekmann D, Hall A. (1992). *Cell* **70**: 401–410.
Riento K, Ridley AJ. (2003). *Nat Rev Mol Cell Biol* **4**: 446–456.
Sahai E, Marshall CJ. (2002). *Nat Rev Cancer* **2**: 133–142.
Sahai E, Olson MF, Marshall CJ. (2001). *EMBO J* **20**: 755–766.
Sampath P, Pollard TD. (1991). *Biochemistry* **30**: 1973–1980.
Sanchez I, Hughes RT, Mayer BJ, Yee K, Woodgett JR, Avruch J *et al*. (1994). *Nature* **372**: 794–798.
Spector I, Shochet NR, Kashman Y, Groweiss A. (1983). *Science* **219**: 493–495.
Subbaramaiah K, Hart JC, Norton L, Dannenberg AJ. (2000). *J Biol Chem* **275**: 14838–14845.
Tanaka H, Yamashita T, Asada M, Mizutani S, Yoshikawa H, Tohyama M. (2002). *J Cell Biol* **158**: 321–329.
Uehata M, Ishizaki T, Satoh H, Ono T, Kawahara T, Morishita T *et al*. (1997). *Nature* **389**: 990–994.
Walker K, Olson MF. (2005). *Curr Opin Genet Dev* **15**: 62–68.
Woods D, Parry D, Cherwinski H, Bosch E, Lees E, McMahon M. (1997). *Mol Cell Biol* **17**: 5598–5611.
Yokoo T, Toyoshima H, Miura M, Wang Y, Iida KT, Suzuki H *et al*. (2003). *J Biol Chem* **278**: 52919–52923.
Yujiri T, Fanger GR, Garrington TP, Schlesinger TK, Gibson S, Johnson GL. (1999). *J Biol Chem* **274**: 12605–12610.
Zhu X, Ohtsubo M, Bohmer RM, Roberts JM, Assoian RK. (1996). *J Cell Biol* **133**: 391–403.